Research Square

Preprints are preliminary reports that have not undergone peer review.
They should not be considered conclusive, used to inform clinical practice,
or referenced by the media as validated information.

Geochemical Contamination, Potential Sources, and Ecological and Human Health Risks in Mining Soils of

Jerome Nworu

sunday.nworu@ebsu.edu.ng

Nigeria Maritime University

Ursula Nworu

Ebonyi State University

Edith Enemose

Nigeria Maritime University

Lucky Arisabor

Nigeria Maritime University

Nwabueze Elom

Alex Ekwueme Federal University, Ndufu-Alike

Research Article

Keywords: Potentially toxic elements (PTEs), Mining soils, Geochemical enrichment, Principal component analysis, Ecological risk, Human health risk, Ebonyi State

Posted Date: November 9th, 2026

DOI: https://doi.org/10.21203/rs.3.rs-11390025/v1

License: This work is licensed under a Creative Commons Attribution 4.0 International License.
Read Full License

Additional Declarations: No competing interests reported.

Geochemical Contamination, Potential Sources, and Ecological and Human Health Risks in Mining Soils of Ebonyi State, Nigeria

[1*]Nworu S. Jerome, [1]Edith A. Enemose, [2]Nworu A. Ursula, [3]Arisabor Lucky and [4]Elom I. Nwabueze

[1]Department of Industrial Chemistry, Nigeria Maritime University, Okerenkoko, Delta, Nigeria
[2]Department of Computer Science, Ebonyi State University Abakaliki, Nigeria
[3]Department of Meteorology and Climate Change, Nigeria Maritime University, Okerenkoko, Delta, Nigeria
[4]Department of Chemistry, Alex-Ekwueme Federal University, Ndufu-Alike, Abakaliki, Nigeria

Corresponding author: Nworu S. Jerome (Sunday.nworu@ebsu.edu.ng; Jerome.nworu@nmu.edu.ng)

Abstract

Mining-induced accumulation of potentially toxic elements (PTEs) threatens soil quality and environmental health, yet integrated assessments across contrasting mineral deposits and mining statuses remain limited. This study investigated the distribution, geochemical enrichment, potential sources, ecological risks and oral human health risks of Cd, Cr, Cu, Ni, Pb and Zn in 120 surface soil samples collected from active and abandoned Pb–Zn and limestone mines in Ebonyi State, Nigeria. Pseudo-total PTE concentrations were determined using aqua-regia digestion and flame atomic absorption spectrophotometry. Contamination indices, ecological and human health risk models, principal component analysis (PCA), PERMANOVA and multivariate regression were applied. Lead and Zn concentrations were highest in active Pb–Zn mines, reaching 4240.13 and 3401.39 mg kg^{-1}, respectively. Thirteen of 18 active–abandoned comparisons were significant after false discovery rate correction ($q < 0.05$). Pollution load indices ranged from 3.78 to 19.34, while potential ecological risk indices ranged from 185.54 to 1124.13, with Ameka active mine exhibiting the greatest cumulative contamination and ecological risk. The first three principal components explained 80.68% of elemental variability, while PERMANOVA confirmed significant differences among sites ($R^2 = 0.516$; $p = 0.0002$). Children's partial oral hazard indices ranged from 0.987 to 2.201, exceeding unity at four locations, with Cd contributing 95.2–98.0% of the calculated hazard. These findings demonstrate persistent contamination in active and abandoned mines and highlight the importance of integrated geochemical assessment, targeted remediation and child-focused exposure monitoring.

Keywords: Potentially toxic elements (PTEs); Mining soils; Geochemical enrichment; Principal component analysis; Ecological risk; Human health risk; Ebonyi State.

1. Introduction

Mining activities contribute substantially to the accumulation of potentially toxic elements (PTEs) in soils through mineral extraction, ore processing, waste disposal and inadequate site rehabilitation. Metallic contaminants are non-biodegradable and may persist in soils for prolonged periods [1–3], potentially degrading soil quality, disrupting microbial processes, impairing ecosystem productivity and increasing human exposure [2–5]. Their distribution and mobility are governed by mineral weathering, sulfide oxidation, adsorption–desorption, precipitation–dissolution and complexation reactions, influenced by soil pH, redox conditions, mineralogy and

organic matter [3, 6]. Oxidation of sulfide-bearing Pb–Zn deposits can release Pb, Zn, Cd and associated elements [7, 8], whereas carbonate-rich limestone environments may favour metal retention through acidity buffering and precipitation. Mining status may further influence contamination patterns: active operations continuously expose mineralized materials, while abandoned mines remain susceptible to weathering, erosion and redistribution of residual contaminants [8, 9]. These contrasting conditions underscore the need to evaluate PTE contamination across different mineral deposits and mining histories. Geochemical indices provide complementary measures of contamination intensity and potential environmental consequences. The contamination factor (CF) and geoaccumulation index (Igeo) assess elemental enrichment relative to background concentrations [10, 11], while the enrichment factor (EF) and potential ecological risk index (PERI) evaluate normalized enrichment and toxicity-weighted ecological risks, respectively [12, 25]. The pollution load index (PLI) and modified degree of contamination (mCd) further characterize cumulative elemental contamination. However, these indices depend on representative geochemical backgrounds and appropriate toxicological parameters, particularly in mineralized environments where natural enrichment may overlap with mining-related inputs. Human health implications also depend on exposure pathways, elemental speciation and toxicological characteristics [13–18]. Complementary statistical approaches, including correlation analysis and principal component analysis (PCA), can identify elemental associations and dominant geochemical variability, supporting the interpretation of potential contamination sources [1, 19]. Nevertheless, statistical associations alone cannot distinguish geological contributions from mining-related inputs without supporting environmental evidence. Integrating geochemical indices, soil properties, multivariate statistics and risk assessment therefore offers a more comprehensive framework for evaluating mining-affected soils.

Ebonyi State, southeastern Nigeria, lies within the Lower Benue Trough, where economically significant Pb–Zn mineralization occurs within Cretaceous sedimentary formations [20]. Previous studies have documented elevated PTE concentrations in soils and contamination of water resources associated with regional mining activities [21–23]. However, integrated comparisons of active and abandoned Pb–Zn and limestone mining environments, incorporating soil physicochemical properties, elemental enrichment, cumulative contamination, ecological risks, multivariate geochemical relationships and human health exposure, remain limited. This knowledge gap constrains understanding of site-specific contamination patterns, persistent legacy pollution and environmental management priorities. Accordingly, this study investigated the distribution, geochemical contamination, potential sources, ecological risks and oral human health risks of Cd, Cr, Cu, Ni, Pb and Zn in soils from six active and abandoned mining locations in Ebonyi State. Specifically, it aimed to (i) characterize soil physicochemical properties and pseudo-total PTE concentrations; (ii) compare elemental distributions between active and abandoned Pb–Zn and limestone mines; (iii) quantify geochemical enrichment and cumulative contamination; (iv) evaluate element-specific and integrated potential ecological risks; (v) investigate elemental associations and potential sources using correlation analysis and PCA; and (vi) assess potential human health risks associated with soil ingestion. The study's contribution lies in integrating geochemical characterization, contamination indices, multivariate statistics and receptor-specific risk assessment within a comparative multi-site framework, providing evidence of site-specific contamination patterns across contrasting mining environments. The findings offer a basis for identifying contamination hotspots, prioritizing environmental monitoring and guiding targeted remediation of mining-affected soils.

Location and geology of the study area

Ebonyi State is located in southeastern Nigeria, within the Lower Benue Trough, a sedimentary basin characterized by Cretaceous geological formations and economically significant mineral deposits [20–22]. The study areas comprise Ameka, Nkpuma Akpatakpa and Ishiagu, representing major mining environments within the State (Fig. 1). Ameka and Nkpuma Akpatakpa are associated with Pb–Zn mineralization, whereas Ishiagu was selected to represent limestone mining activities. These locations provide contrasting geological and mining conditions for evaluating the distribution and contamination characteristics of potentially toxic elements (PTEs). Geologically, the Lower Benue Trough consists predominantly of Cretaceous sedimentary sequences, including shale, sandstone, limestone and associated mineralized formations [20–22]. Pb–Zn mineralization in the Abakaliki region occurs principally as hydrothermal vein and fracture-filling deposits associated with the sedimentary formations. Weathering and oxidation of sulfide-bearing minerals may release Pb, Zn, Cd and other associated elements into surrounding soils, particularly where mineral extraction and waste disposal expose previously buried materials to atmospheric conditions [7, 8]. In contrast, limestone-bearing environments are characterized by carbonate-rich geological materials that may influence soil acidity, metal retention and precipitation reactions [3, 6]. The surface soils in these mining environments are influenced by weathering of the underlying geological formations and disturbances associated with mineral extraction, processing and waste accumulation. Active mining locations experience continued exposure of mineralized materials and redistribution of mine wastes, whereas abandoned locations remain subject to prolonged weathering, erosion and leaching of residual contaminants [8, 9]. These processes may produce variations in soil physicochemical properties and PTE concentrations across the investigated locations. Understanding the geological characteristics and mining histories of these environments is therefore essential for interpreting elemental distributions, geochemical enrichment and potential ecological risks.

Materials and methods

Soil sampling strategy and laboratory analysis

The sampling locations were selected to represent differences in mineral deposit type, mining status and geographical distribution within Ebonyi State. Three mining districts, namely Ameka, Nkpuma Akpatakpa and Ishiagu, were investigated. Within each district, one active and one abandoned mining location were selected, giving six sampling sites. The sites were designated as Ameka Active Mine (AA), Ameka Abandoned Mine (AB), Nkpuma Akpatakpa Active Mine (NA), Nkpuma Akpatakpa Abandoned Mine (NB), Ishiagu Active Mine (IA) and Ishiagu Abandoned Mine (IB). The active and abandoned locations were selected to provide a comparative basis for evaluating PTE contamination associated with ongoing mineral extraction and historical mining activities. Their geographical coordinates are presented in Table 1.

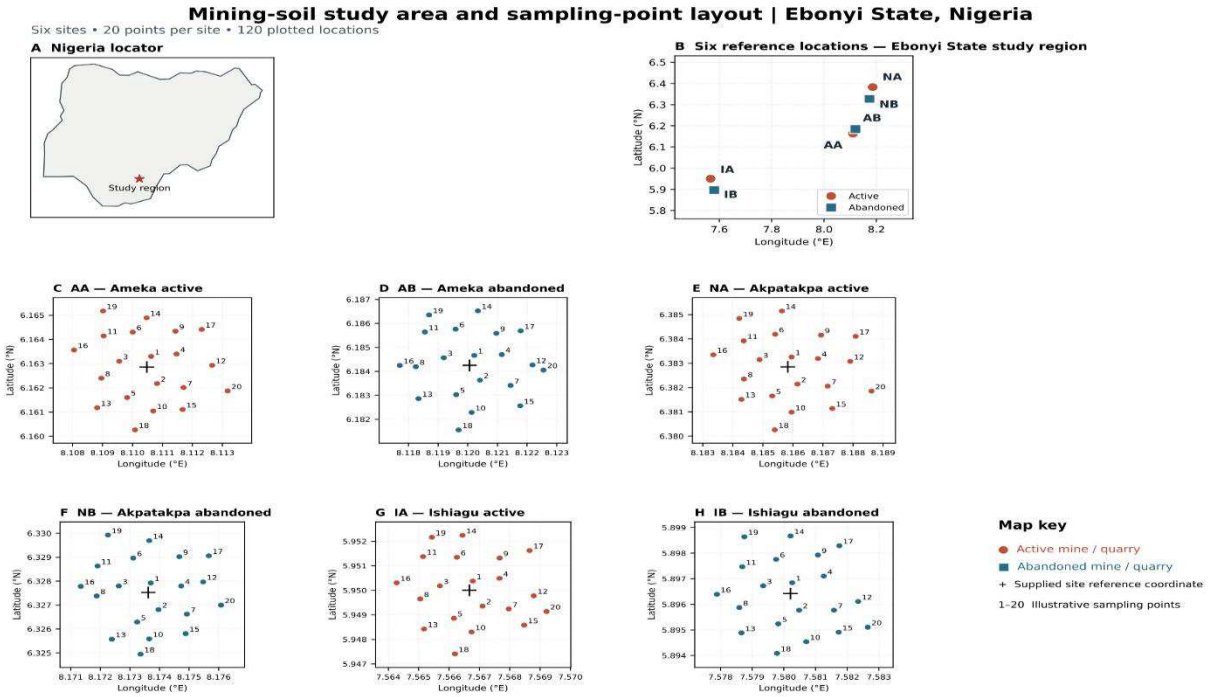


Fig. 1: Geographic distribution of active and abandoned mining locations in Ebonyi State, southeastern Nigeria. The map illustrates the study region within Nigeria and the spatial distribution of six mining locations: Ameka active (AA), Ameka abandoned (AB), Nkpuma Akpatakpa active (NA), Nkpuma Akpatakpa abandoned (NB), Ishiagu active (IA), and Ishiagu abandoned (IB). Twenty sampling positions are illustrated at each location, giving a total of 120 points.Sampling design and soil collection

Table 1.

Geographic coordinates and distribution of soil sampling locations across active and abandoned mining environments in Ebonyi State, Nigeria

Locations	Latitude (°N)	Longitude (°E)	Coordinates (DMS)
Ameka, Ezza South (AA)	6.16286	8.11048	6°09′46.30″N, 8°06′37.73″E
Ameka (AA) control	6.02134	8.10536	6°01′16.82″N, 8°06′19.30″E
Ameka, Ezza South (AB)	6.18425	8.12006	6°11′03.30″N, 8°07′12.22″E
Ameka (AB) control	6.03231	7.86738	6°01′56.32″N, 7°52′02.57″E
Akpatakpa, Izzi (NA)	6.38285	8.18583	6°22′58.26″N, 8°11′08.99″E
Akpatakpa (NA) control	5.98351	7.93682	5°59′00.64″N, 7°56′12.55″E
Akpatakpa, Izzi (NB)	6.32753	8.17362	6°19′39.11″N, 8°10′25.03″E
Akpatakpa (NB) control	6.10362	8.06374	6°06′13.03″N, 8°03′49.46″E
Ishiagu, Ivo (IA)	5.95000	7.56667	5°57′00.00″N, 7°34′00.01″E
Ishiagu (IA) control	5.77352	7.48829	5°46′24.67″N, 7°29′17.84″E
Ishiagu, Ivo (IB)	5.89642	7.58021	5°53′47.11″N, 7°34′48.76″E
Ishiagu (IB) control	5.72135	7.94522	5°43′16.86″N, 7°56′42.79″E

AA = Ameka Active Mine; AB = Ameka Abandoned Mine; NA = Nkpuma Akpatakpa Active Mine; NB = Nkpuma Akpatakpa Abandoned Mine; IA = Ishiagu Active Mine; IB = Ishiagu Abandoned Mine. Control denotes the corresponding reference soil sampling location.

Soil sampling was conducted between 12 and 30 October 2025 using a stratified composite sampling design consistent with established soil quality assessment principles [26]. Twenty composite surface soil samples were collected from each of the six mining locations at a depth of 5–10 cm, yielding 120 samples. Sampling points were distributed across the mining environments to capture spatial variability in soil properties and potentially toxic element (PTE) concentrations. The selected depth represents the near-surface soil layer susceptible to mining disturbances, atmospheric deposition and contaminant accumulation. Samples were collected in labelled polyethylene containers and transported to the laboratory, where they were air-dried at 25–30 °C, cleared of extraneous materials, disaggregated, sieved to <250 µm, homogenized and stored in polyethylene containers until analysis. Pseudo-total concentrations of Cd, Cr, Cu, Ni, Pb and Zn were determined by aqua-regia digestion followed by flame atomic absorption spectrophotometry (FAAS) [27]. Approximately 0.5 g of homogenized soil was treated with 20 mL of freshly prepared aqua regia ($HCl:HNO_3$ 3:1, *v/v*), predigested for 24 h and heated at approximately 90 °C for 1 h. After cooling, the digests were filtered through Whatman No. 42 filter paper and diluted to 50 mL with deionized water. Elemental concentrations were measured using a GBC XplorAA flame atomic absorption spectrophotometer. Aqua-regia extraction provides pseudo-total rather than absolute total concentrations because metals incorporated within resistant silicate minerals may not be completely recovered [27, 31]. Analytical quality assurance and quality control included reagent blanks, instrument calibration, control samples, replicate analyses and certified reference material (NIST 2710a). Calibration coefficients of determination (R^2) ranged from 0.998 to 0.999, while analytical recoveries exceeded 88%. Precision was assessed through replicate measurements. Elemental concentrations were expressed as mg kg^{-1} dry soil and subsequently used for geochemical characterization, contamination-index calculations and statistical analyses.

Recovery and precision were calculated using:

$$\text{Recovery (percent)} = \frac{C_m}{C_c} \times 100 \quad (1)$$

$$\text{RSD (percent)} = \frac{\text{SD}}{\overline{C}} \times 100 \quad (2)$$

where C_m is the measured concentration, C_c is the certified concentration, SD is the standard deviation of replicate measurements and $\overline{C}$ is the mean measured concentration.

Determination of soil physicochemical properties

Soil physicochemical characteristics were assessed to evaluate variations in soil conditions and their potential influence on the distribution of potentially toxic elements (PTEs) across the investigated mining environments. Soil pH was determined electrometrically using a calibrated digital pH meter in suspensions prepared separately with deionized water and 0.01 M calcium chloride ($CaCl_2$) solution. For pH determination in water, 10.0 g of air-dried soil was mixed with 25 mL of deionized water at a soil-to-solution ratio of 1:2.5 (w/v) [6, 24]. The suspension was stirred, allowed to equilibrate and measured using the calibrated electrode. The $CaCl_2$ determination was performed separately using the laboratory's recorded soil-to-solution ratio and equilibration conditions, consistent with established electrometric soil pH measurement principles [28, 29]. Soil organic matter (SOM) was estimated from soil organic carbon determined by the Walkley–Black wet oxidation method [30], Iron (Fe) and manganese (Mn) concentrations were

determined by flame atomic absorption spectrophotometry (FAAS) following acid extraction of homogenized soil samples [31]. The physicochemical and elemental data were subsequently used to examine variations between active and abandoned Pb–Zn and limestone mining environments. Relationships among soil pH, SOM, Fe, Mn and PTE concentrations were evaluated statistically to investigate potential geochemical controls on elemental distribution.

Assessment of PTE contamination and geochemical enrichment

To evaluate contamination severity, the contamination factor (CF) and geo-accumulation index (Igeo) were evaluated.

Contamination factor

The contamination factor was calculated as:

$$CF_i = \frac{C_i}{B_i} \quad (3)$$

where C_i represents the measured pseudo-total concentration of element i and B_i represents its corresponding geochemical background concentration. The conventional contamination categories are CF < 1 (low), 1–3 (moderate), 3–6 (considerable) and CF ≥ 6 (very high contamination) [25].

Pollution load index (PLI)

The pollution load index (PLI) was employed to assess the cumulative contamination of Cd, Cr, Cu, Ni, Pb and Zn across the six mining environments. The index integrates individual contamination factors (CFs) into a single measure of overall soil contamination. Following Tomlinson et al. [32] and Udo et al. [25], PLI was calculated as:

$$PLI = (CF_1 \times CF_2 \times \ldots\ldots CF_n)^{1/n} \quad (4)$$

where CF_i represents the contamination factor of the ith element and n is the number of elements investigated (n = 6). PLI values below 1 indicate no overall enrichment relative to the selected background, a value of 1 represents background-equivalent contamination, and values above 1 indicate cumulative enrichment. Higher PLI values reflect greater overall contamination intensity across the mining locations.

Modified degree of contamination (mCd)

The modified degree of contamination (mCd) was used to evaluate the combined contamination intensity of the investigated PTEs. The index represents the arithmetic mean of individual contamination factors and provides a complementary assessment of overall metal enrichment. Following Udo et al. [25] and Abrahim and Parker [33], mCd was calculated as:

$$mCd = \frac{\sum_{i-1}^{n} C_f^i}{n} \quad (5)$$

where CF_i is the contamination factor of the ith element and n is the total number of elements analyzed (n = 6). The mCd values were classified according to Abrahim and Parker [30] as follows: mCd < 1.5, nil to very low contamination; 1.5 ≤ mCd < 2, low contamination; 2 ≤ mCd < 4, moderate contamination; 4 ≤ mCd < 8, high contamination; 8 ≤ mCd < 16, very high

contamination; 16 ≤ mCd < 32, extremely high contamination; and mCd ≥ 32, ultra-high contamination. The resulting indices were used to compare cumulative PTE contamination between active and abandoned Pb–Zn and limestone mining environments.

Geoaccumulation index

The geoaccumulation index was calculated according to Müller [10]:

$$I_{\text{geo}} = \log_2\left(\frac{C_i}{1.5B_i}\right) \quad (6)$$

The factor 1.5 accounts for possible natural variability in background concentrations. The resulting Igeo values were classified into seven categories ranging from uncontaminated to extremely contaminated.

Enrichment factor (EF)

The enrichment factor (EF) was employed to assess the relative enrichment of Cd, Cr, Cu, Ni, Pb and Zn in soils from active and abandoned mining environments. The index normalizes the concentration of each investigated element against a suitable reference element and compares the resulting ratio with corresponding background values. Following established geochemical normalization approaches [34–36], EF was calculated as:

$$EF_i = \frac{(C_i/C\text{ref})\text{sample}}{(B_i/B\text{ref})\text{background}} \quad (7)$$

where (C_i) and (C_{ref}) represent the concentrations of the investigated element and reference element in the soil sample, respectively, while (B_i) and (B_{ref}) denote their corresponding background concentrations. Iron (Fe) was considered as the reference element because of its established application in geochemical normalization. EF values were classified as minimal (< 2), moderate (2–< 5), significant (5–< 20), very high (20–< 40) and extremely high (≥ 40) enrichment [32]. The resulting values were used to compare elemental enrichment across the six mining environments. Interpretations considered the possible influence of natural mineralization, soil geochemistry and mining-related disturbances.

Potential ecological risk assessment

Potential ecological risk was evaluated using the approach originally proposed by Håkanson [12]. The element-specific ecological risk factor was calculated as:

$$E_r^i = T_r^i \times CF_i \quad (8)$$

The cumulative potential ecological risk index was calculated as:

$$PERI = \sum i = 1^n E_r^i \quad (9)$$

where T_r^i represents the toxic-response factor for element i, and CF_i is the corresponding contamination factor.

Human health risk assessment

Human health risk assessment was designed to estimate potential exposure to soil-associated PTEs in children and adults using established exposure assessment principles [13–15].

Exposure assessment

The average daily dose (ADD) associated with incidental soil ingestion was calculated as:

$$ADD = \frac{C_s \times IngR \times EF \times ED \times CF_u}{BW \times AT} \quad (10)$$

where C_s is soil PTE concentration (mg kg^{-1}), $IngR$ is soil ingestion rate (mg day^{-1}), EF is exposure frequency (days year^{-1}), ED is exposure duration (years), BW is body weight (kg), AT is averaging time (days), and CF_u is the unit conversion factor (10^{-6} kg mg^{-1}). Screening parameters are soil ingestion rates of 200 and 100 mg day^{-1} and body weights of 15 and 70 kg for children and adults, respectively. Exposure frequency was set at 350 days year^{-1}, with exposure durations of 6 years for children and 30 years for adults.

Non-carcinogenic risk assessment

For elements with appropriate oral reference doses, the hazard quotient was calculated as:

$$HQ_i = \frac{ADD_i}{RfD_i} \quad (11)$$

The cumulative hazard index was estimated as:

$$HI = \sum i = 1^n HQ_i \quad (12)$$

An HQ or HI exceeding unity was interpreted as indicating a potential concern requiring further investigation rather than evidence that adverse health effects would necessarily occur. For Pb, which does not have a generally accepted health-protective oral reference dose, a separate screening approach was employed [17].

Carcinogenic risk assessment

Carcinogenic risk (CR) was estimated using:

$$CR = ADD \times CSF \quad (13)$$

where ADD = the average daily dose and CSF = cancer slope factor (mg/kg-day)$^{-1}$. ADD was given from eqn. (10). The CSF = cancer slope factor (mg/kg-day)$^{-1}$ had the following values for the toxic PTEs: 8.5, 41, 6.1, and 0.84 (kg/day/mg) for Pb, Cr, Cd, and Ni, respectively [40].

Statistical analysis

Following established environmental statistical approaches [37, 38], statistical analyses were performed on 120 soil samples collected from six active and abandoned mining sites (n = 20 per site). Results were expressed as mean ± standard deviation (SD). Differences in soil physicochemical properties among sites were assessed using one-way analysis of variance

(ANOVA), followed by Fisher's least significant difference (LSD) test. Active–abandoned differences in potentially toxic element (PTE) concentrations within each mining district were evaluated using Welch's t-test on $\log_{10}$-transformed data, with Hedges' g effect sizes, geometric mean ratios and 95% confidence intervals (CIs). Pearson's correlation analysis examined relationships among PTEs and soil properties. Principal component analysis (PCA) was applied to $\log_{10}$-transformed, standardized PTE concentrations to identify elemental associations and patterns of geochemical variability. Multivariate differences among sites were evaluated using Euclidean-distance-based permutational multivariate analysis of variance (PERMANOVA; 4,999 permutations), complemented by a permutation-based multivariate dispersion test. Site-adjusted multiple linear regression, incorporating site fixed effects and HC3 robust standard errors, was used to investigate associations between PTE concentrations and soil pH, organic matter, Fe and Mn. Element-specific contributions to the non-carcinogenic hazard index (HI) and sample-level HI exceedance frequencies were also determined. Statistical significance was assessed at $p < 0.05$, with Benjamini–Hochberg false discovery rate correction applied to multiple comparisons ($q < 0.05$).

Results and Discussion

Soil Physicochemical Characteristics and PTE Distribution

The physicochemical characteristics of soils from the six mining locations exhibited significant spatial variability (Table 2), reflecting differences in geological settings, mineral composition and mining-related disturbances. Soil pH measured in water ranged from 5.56 ± 0.16 at Nkpuma Akpatakpa abandoned mine (NB) to 6.92 ± 0.20 at Ishiagu abandoned mine (IB), with significant differences among locations ($p < 0.001$). The Ameka and Nkpuma Akpatakpa soils were predominantly acidic, whereas the Ishiagu soils approached neutrality. This contrast is consistent with the different geological environments, particularly the potential for sulfide oxidation in Pb–Zn mineralized areas and carbonate buffering in limestone-bearing formations. Oxidation of sulfide minerals can generate acidity and promote metal dissolution, whereas carbonate minerals may neutralize acidity and favour metal retention through adsorption and precipitation [3, 6]. Nevertheless, the observed pH differences cannot independently establish these mechanisms without supporting mineralogical or pore-water analyses. Soil organic matter (SOM) varied significantly ($p < 0.001$), with the highest concentrations at NA (2.06 ± 0.38%) and AA (1.85 ± 0.54%), compared with the lowest at IB (0.70 ± 0.15%). Similarly, Fe concentrations were substantially higher at AA (774.67 ± 64.68 mg kg^{-1}) and NA (670.41 ± 105.48 mg kg^{-1}) than at IB (49.55 ± 21.91 mg kg^{-1}), while Mn ranged from 1512.47 ± 270.58 to 2055.14 ± 128.34 mg kg^{-1}. These variations indicate heterogeneous soil matrices that may influence metal adsorption, complexation and retention. Organic matter can provide reactive binding sites, whereas Fe–Mn-bearing phases may participate in the sequestration and redistribution of trace elements [3]. However, the measured Fe and Mn concentrations represent operationally extracted elemental concentrations rather than direct measurements of reactive oxide phases; their roles as sorbents therefore remain plausible interpretations rather than demonstrated mechanisms.

Table 2.

Physicochemical characteristics of soils from active and abandoned mining sites in Ebonyi State, Nigeria

Site	pH (H_2O)	pH ($CaCl_2$)	SOM (%)	Fe (mg/kg)	Mn (mg/kg)

AA	5.84 ± 0.16^{b}	5.99 ± 0.26^{b}	1.85 ± 0.54^{a}	774.67 ± 64.68^{a}	2055.14 ± 128.34^{a}
AB	5.67 ± 0.12^{cd}	5.79 ± 0.20^{c}	1.15 ± 0.42^{c}	363.62 ± 211.14^{c}	1995.08 ± 104.50^{a}
NA	5.72 ± 0.16^{c}	5.78 ± 0.18^{c}	2.06 ± 0.38^{a}	670.41 ± 105.48^{b}	1986.31 ± 113.13^{a}
NB	5.56 ± 0.16^{d}	5.68 ± 0.28^{c}	1.39 ± 0.27^{b}	181.49 ± 68.73^{d}	1871.09 ± 122.93^{b}
IA	6.88 ± 0.21^{a}	6.04 ± 0.17^{b}	1.27 ± 0.29^{bc}	108.86 ± 32.21^{e}	1962.04 ± 78.76^{ab}
IB	6.92 ± 0.20^{a}	6.52 ± 0.46^{a}	0.70 ± 0.15^{d}	49.55 ± 21.91^{e}	1512.47 ± 270.58^{c}
LSD (0.05)	0.108	0.173	0.229	65.767	93.868
ANOVA F	265.38	23.97	36.18	166.80	34.81
ANOVA p	<0.001	<0.001	<0.001	<0.001	<0.001

Values are presented as mean ± standard deviation (n = 20). Means within the same column sharing at least one superscript letter (a–e) are not significantly different ($p \geq 0.05$), whereas means with no common superscript letter differ significantly ($p < 0.05$), according to Fisher's least significant difference (LSD) test following one-way ANOVA.

Table 3.

Concentrations of potentially toxic elements in active and abandoned mining soils of Ebonyi State, Nigeria (mg kg^{-1})

Site	Cd	Cr	Cu	Ni	Pb	Zn
AA	16.23 ± 9.20	141.21 ± 49.65	196.06 ± 82.39	99.03 ± 30.26	4240.13 ± 2149.82	2834.05 ± 2057.28
AB	7.35 ± 4.44	87.98 ± 39.67	79.98 ± 35.10	72.55 ± 17.73	1929.60 ± 1891.48	948.84 ± 689.94
NA	15.45 ± 7.77	159.07 ± 55.21	180.60 ± 89.31	102.00 ± 27.21	3892.85 ± 1930.85	3401.39 ± 2636.70
NB	16.87 ± 9.07	85.41 ± 18.62	100.28 ± 12.26	68.56 ± 25.30	1771.67 ± 1432.00	1103.57 ± 825.89
IA	9.09 ± 7.21	71.39 ± 26.16	57.64 ± 11.98	52.87 ± 22.87	95.39 ± 97.78	322.92 ± 103.04
IB	7.53 ± 4.03	54.95 ± 23.78	30.88 ± 7.53	46.51 ± 12.33	248.63 ± 366.53	184.44 ± 78.83

Values are expressed as mean ± SD (n = 20 per site). AA and AB represent active and abandoned Ameka Pb–Zn mines; NA and NB, active and abandoned Nkpuma Akpatakpa Pb–Zn mines; and IA and IB, active and abandoned Ishiagu limestone mines, respectively.

The concentrations of Cd, Cr, Cu, Ni, Pb and Zn also varied markedly among mining environments (Table 3; Fig. 3). The Pb–Zn mining locations generally exhibited substantially higher Pb and Zn concentrations than the limestone locations, consistent with the mineralization characteristics of the Lower Benue Trough (Olade and Morton, 1985). Mean Pb concentrations were highest at AA (4240.13 ± 2149.82 mg kg^{-1}), followed by NA (3892.85 ± 1930.85 mg kg^{-1}), whereas IA recorded the lowest concentration (95.39 ± 97.78 mg kg^{-1}). Similarly, Zn concentrations were highest at NA (3401.39 ± 2636.70 mg kg^{-1}) and AA (2834.05 ± 2057.28 mg kg^{-1}), compared with 184.44 ± 78.83 mg kg^{-1} at IB. These pronounced differences suggest substantial accumulation of Pb and Zn within the mineralized districts, potentially associated with ore extraction, waste-rock exposure, mineral weathering and redistribution of mine-derived particulates. Previous investigations in southeastern Nigeria have likewise identified mining-associated PTE contamination in Pb–Zn environments, supporting the regional significance of these observations [9, 21, 22].

Other PTEs exhibited more complex distributions. Cd concentrations were highest at NB (16.87 ± 9.07 mg kg^{-1}), followed by AA (16.23 ± 9.20 mg kg^{-1}) and NA (15.45 ± 7.77 mg kg^{-1}), indicating that elevated Cd was not confined to active mining locations. Chromium reached its highest mean concentration at NA (159.07 ± 55.21 mg kg^{-1}), while Cu and Ni were highest at AA (196.06 ± 82.39 and 99.03 ± 30.26 mg kg^{-1}, respectively) or NA (180.60 ± 89.31 and 102.00 ± 27.21 mg kg^{-1}, respectively). The comparatively elevated Cd at NB, despite its abandoned status, suggests

that residual mine materials and continuing geochemical weathering may sustain contamination after extraction activities cease. This interpretation is consistent with Cánovas et al. [2], who investigated the potential release of metal(loid)s from wastes deposited at historical abandoned sulfide mines, demonstrating the importance of evaluating legacy mine materials rather than assuming that abandonment eliminates contamination.

Table 4.
Pearson correlation coefficients among soil properties and potentially toxic elements

Variable	pH-H_2O	pH-$CaCl_2$	SOM	Fe	Mn	Cd	Cr	Cu	Ni	Pb	Zn
pH-H_2O	—										
pH-$CaCl_2$	0.62**	—									
SOM	-0.46**	-0.36**	—								
Fe	-0.54**	-0.31**	0.63**	—							
Mn	-0.41**	-0.55**	0.50**	0.50**	—						
Cd	-0.29**	-0.18*	0.30**	0.24**	0.11	—					
Cr	-0.49**	-0.35**	0.52**	0.51**	0.37**	0.24**	—				
Cu	-0.60**	-0.42**	0.62**	0.68**	0.50**	0.34**	0.53**	—			
Ni	-0.51**	-0.21*	0.41**	0.53**	0.27**	0.14	0.36**	0.46**	—		
Pb	-0.75**	-0.39**	0.56**	0.69**	0.34**	0.33**	0.47**	0.59**	0.56**	—	
Zn	-0.64**	-0.39**	0.63**	0.69**	0.44**	0.28**	0.56**	0.66**	0.51**	0.67**	—

*Pearson r; * $p < 0.05$, ** $p < 0.01$ (two-sided, unadjusted). Metal concentrations were $\log_{10}$-transformed before correlation; Fe, Mn, SOM and pH were analyzed on their original scales. Values below detection limits coded as zero were replaced by half the smallest positive concentration within the analyzed group.*

Statistical comparisons further confirmed that active–abandoned differences were element- and location-dependent (Table 5). Thirteen of the 18 comparisons remained significant following Benjamini–Hochberg correction ($q < 0.05$). At Ameka, all six elements were significantly higher at AA than AB, with active-to-abandoned geometric mean ratios of 3.29 for Pb, 2.95 for Zn and 2.70 for Cu. Corresponding Hedges' g values of 1.23, 1.39 and 1.68 indicate substantial standardized differences. At Nkpuma Akpatakpa, Cr, Cu, Ni, Pb and Zn were significantly elevated at NA relative to NB, whereas Cd showed no significant difference ($q = 0.813$). In contrast, only Cu and Zn differed significantly between IA and IB, with ratios of 1.88 and 1.79, respectively. Notably, Pb exhibited a lower geometric mean at IA than IB (ratio = 0.48), although this difference was not statistically significant after adjustment ($q = 0.0915$). Collectively, these results indicate that active mining locations generally exhibited greater elemental accumulation within the investigated Pb–Zn districts, whereas the limestone locations displayed less consistent differences. Because each district contained only one active and one abandoned location, these comparisons represent site-specific contrasts rather than independently replicated estimates of a general mining-status effect. The considerable standard deviations associated with Pb, Zn and Cd also indicate substantial within-site heterogeneity, potentially reflecting uneven distribution of mineralized fragments, tailings and contaminated soil particles. Such heterogeneity is important for environmental assessment because site-average concentrations may obscure localized contamination. The combined concentration and statistical results therefore demonstrate that geological setting and mining conditions are central to understanding PTE distributions across the studied environments.

Table 5.
Comparison of PTE concentrations between active and abandoned mining sites.

Pair	PTE	Ratio (95% CI)	Hedges' g	q
AA vs AB	Cd	2.13 (1.36–3.33)	1.06	0.00238

AA vs AB	Cr	1.68 (1.25–2.26)	1.09	0.00196
AA vs AB	Cu	2.70 (1.86–3.93)	1.68	4.70×10^{-5}
AA vs AB	Ni	1.35 (1.14–1.60)	1.13	0.00148
AA vs AB	Pb	3.29 (1.78–6.08)	1.23	0.000976
AA vs AB	Zn	2.95 (1.81–4.82)	1.39	0.000300
NA vs NB	Cd	0.94 (0.63–1.40)	−0.09	0.813
NA vs NB	Cr	1.71 (1.29–2.28)	1.20	0.00134
NA vs NB	Cu	1.56 (1.15–2.12)	0.94	0.00887
NA vs NB	Ni	1.53 (1.25–1.88)	1.31	0.000485
NA vs NB	Pb	2.67 (1.67–4.26)	1.32	0.000485
NA vs NB	Zn	2.81 (1.64–4.81)	1.20	0.000976
IA vs IB	Cd	1.09 (0.70–1.71)	0.13	0.769
IA vs IB	Cr	1.35 (0.94–1.95)	0.52	0.123
IA vs IB	Cu	1.88 (1.61–2.20)	2.52	1.57×10^{-8}
IA vs IB	Ni	1.01 (0.71–1.44)	0.02	0.951
IA vs IB	Pb	0.48 (0.21–1.07)	−0.58	0.0915
IA vs IB	Zn	1.79 (1.43–2.23)	1.65	4.56×10^{-5}

AA–AB = Ameka active–abandoned; NA–NB = Nkpuma Akpatakpa active–abandoned; IA–IB = Ishiagu active–abandoned. Ratio = active/abandoned geometric mean concentration; CI = confidence interval; Hedges' g = standardized effect size; q = Benjamini–Hochberg-adjusted p-value. Statistical significance was established at q < 0.05. Each site comprised 20 soil samples.

Table 6.

Integrated contamination and potential ecological risk indices of mining soils in Ebonyi State, Nigeria

Site	PLI	mCd	PERI
AA	19.34 ± 5.09	31.83 ± 10.33	1124.13 ± 406.73
AB	8.01 ± 2.70	14.59 ± 7.64	438.19 ± 238.64
NA	15.23 ± 3.31	30.90 ± 10.36	695.48 ± 195.33
NB	8.47 ± 2.02	12.87 ± 5.22	430.87 ± 146.25
IA	3.78 ± 0.92	4.90 ± 0.84	185.54 ± 88.87
IB	4.09 ± 1.73	5.27 ± 1.94	240.05 ± 94.43

Values are expressed as mean ± standard deviation (n = 20 per site). PLI = pollution load index; mCd = modified degree of contamination; PERI = potential ecological risk index. AA and AB represent active and abandoned Ameka Pb–Zn mines; NA and NB, active and abandoned Nkpuma Akpatakpa Pb–Zn mines; and IA and IB, active and abandoned Ishiagu limestone mines, respectively.

Geochemical contamination and enrichment patterns

The contamination factor (CF), geoaccumulation index (Igeo) and enrichment factor (EF) provided complementary assessments of elemental accumulation relative to the selected background soils (Tables 7–9; Figs. 4–6). CF values revealed particularly pronounced enrichment of Pb and Zn in the Pb–Zn mining districts. At AA, Pb and Zn recorded CF values of 78.23 and 57.29, respectively, compared with 74.65 and 73.24 at NA. These values greatly exceeded the conventional threshold of CF ≥ 6 for very high contamination, indicating substantial accumulation relative to the corresponding reference soils. Lead also exhibited high CF values at AB (42.93) and NB (30.84), demonstrating that considerable contamination persisted at abandoned locations. In contrast, the

limestone sites generally showed lower Pb enrichment, particularly IA (CF = 2.59). The persistence of elevated Pb and Zn in both active and abandoned Pb–Zn environments is consistent with the regional mineralization and the potential long-term influence of exposed ore-bearing materials [9, 20]. Geoaccumulation indices corroborated the CF results while accounting for natural variability in background concentrations. At AA, Pb and Zn exhibited Igeo values of 5.46 and 4.88, respectively, indicating extreme Pb accumulation and strong-to-extreme Zn accumulation. Comparable values were recorded at NA (Pb = 5.44; Zn = 5.11), confirming that these two active Pb–Zn locations represented the most strongly enriched environments. Although lower than their active counterparts, the abandoned locations also exhibited substantial accumulation, with Pb Igeo values of 4.02 at AB and 3.89 at NB. Cadmium and Cu displayed strong accumulation at AA (Igeo = 3.26 and 3.44, respectively), whereas Ni generally showed lower accumulation. These differences indicate that the contamination pattern was not uniform across elements, reinforcing the importance of element-specific assessment alongside cumulative pollution indices. Fe-normalized enrichment factors further distinguished relative elemental enrichment patterns. Pb and Zn exhibited the highest EF values at NA (18.51 and 18.10, respectively), followed by AA (17.28 and 12.44), corresponding to significant enrichment under the adopted classification scheme. At AB and NB, Pb and Zn also exhibited appreciable enrichment, whereas most other elements showed minimal to moderate EF values. The close correspondence between elevated Pb–Zn concentrations, CF, Igeo and EF strengthens the interpretation that Pb–Zn mineralization and mining-related disturbances are important influences on the observed contamination patterns. However, EF does not independently distinguish anthropogenic inputs from natural ore-associated enrichment, particularly in mineralized geological settings [35, 36].

Table 7.

Contamination factors (CF) of PTEs in active and abandoned mining soils of Ebonyi State, Nigeria.

Site	Cd (CF)	Cr (CF)	Cu (CF)	Ni (CF)	Pb (CF)	Zn (CF)	Interpretation
AA	17.82	15.69	17.54	4.41	78.23	57.29	5/6 very high CF
AB	4.22	9.23	9.56	2.26	42.93	19.32	4/6 very high CF
NA	3.77	10.96	14.64	8.14	74.65	73.24	5/6 very high CF
NB	6.17	5.07	6.92	4.63	30.84	23.56	4/6 very high CF
IA	3.79	8.32	3.79	3.12	2.59	7.77	2/6 very high CF
IB	4.85	6.66	3.26	5.02	7.01	4.80	2/6 very high CF

CF = concentration in an individual mining-soil sample divided by the corresponding site-matched control-soil mean. Values shown are the means of sample-level CFs (n = 20/site). Conventional CF classes: <1, low; 1–<3, moderate; 3–<6, considerable; ≥6, very high contamination. The interpretation column gives the number of elements with very high CF.

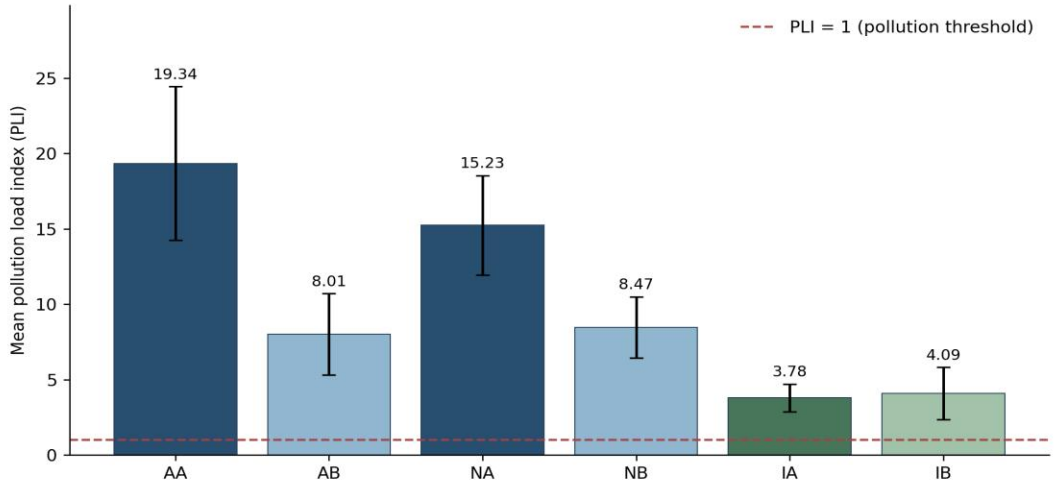


Fig. 2: Variation in mean pollution load index (PLI) across six mining sites in Ebonyi State. Error bars represent standard deviations (n = 20 per site). The dashed horizontal line denotes PLI = 1. AA/AB = Ameka active/abandoned; NA/NB = Nkpuma Akpatakpa active/abandoned; IA/IB = Ishiagu active/abandoned.

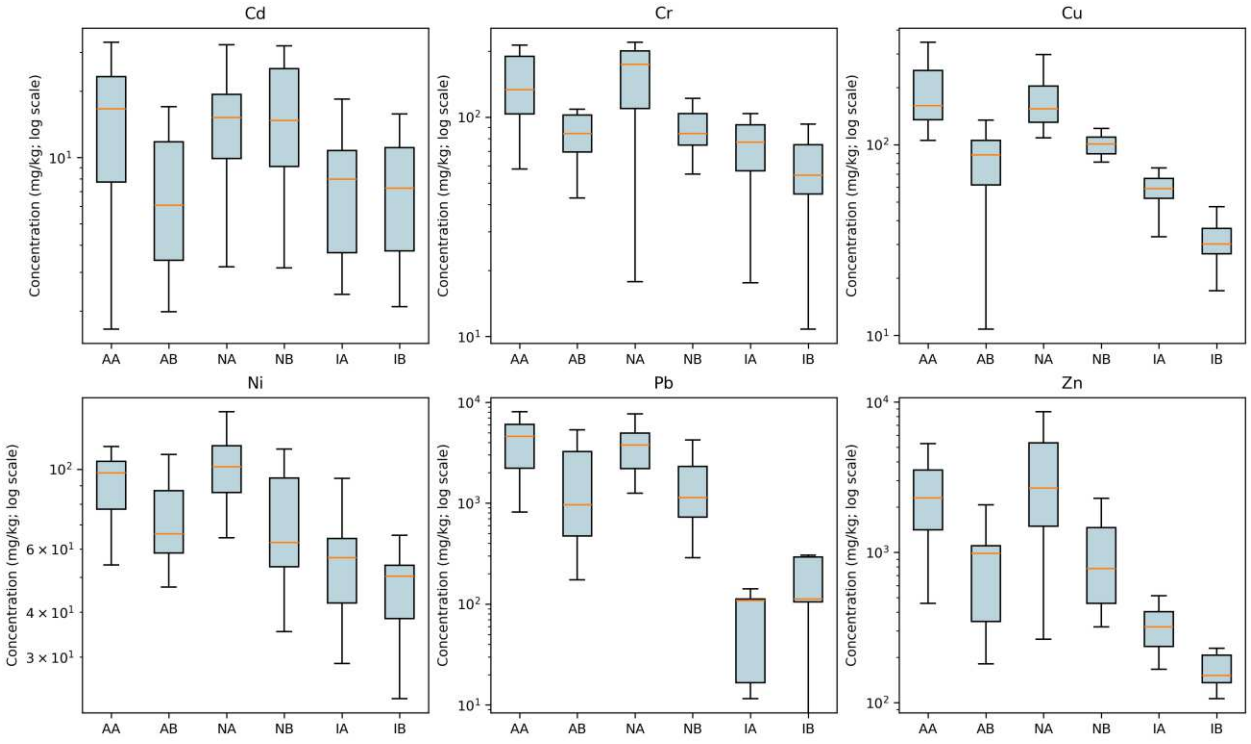


Fig. 3: Distributions of Cd, Cr, Cu, Ni, Pb and Zn across the six mining sites.

The selection of Fe as the normalizing element also requires consideration. Although Fe is commonly employed in geochemical normalization, its concentrations varied substantially among the investigated sites, suggesting that differences in Fe-bearing mineral abundance or extraction behaviour could influence EF estimates. Consequently, EF values should be interpreted alongside CF, Igeo and geological evidence rather than as definitive measures of anthropogenic contamination. This caution is consistent with Reimann and de Caritat [35], who identified important limitations in enrichment-factor approaches, particularly where reference-element behaviour and natural geochemical variability are insufficiently constrained. The three indices consistently identified AA and NA as strongly enriched Pb–Zn mining environments, with persistent but generally lower contamination at AB and NB. The limestone locations displayed comparatively lower enrichment, although individual elements remained elevated relative to their reference soils. The agreement among multiple indices supports the identification of priority monitoring locations, while their common dependence on background concentrations highlights the importance of reliable, geologically representative reference soils. Similar integrated pollution-index approaches have been applied in Nigerian contaminated soils, including the investigation by Udo et al. [25], although differences in pollution sources, reference conditions and analytical procedures limit direct numerical comparison of index magnitudes.

Table 8.

Geoaccumulation index (Igeo) of potentially toxic elements in mining soils of Ebonyi State, Nigeria

Site	Cd	Cr	Cu	Ni	Pb	Zn
AA	3.26	3.29	3.44	1.50	5.46	4.88
AB	1.23	2.46	2.42	0.55	4.02	3.33
NA	1.12	2.72	3.07	2.39	5.44	5.11
NB	1.79	1.72	2.20	1.54	3.89	3.61
IA	0.96	2.33	1.30	0.83	0.04	2.30
IB	1.45	1.95	1.08	1.68	1.64	1.58

Values represent mean Igeo (n = 20 per site, except Pb at IB, n = 18). Igeo ≤ 0 indicates unpolluted; 0–1, unpolluted to moderately polluted; 1–2, moderately polluted; 2–3, moderately to strongly polluted; 3–4, strongly polluted; 4–5, strongly to extremely polluted; and > 5, extremely polluted.

Table 9.

Fe-normalized enrichment factors (EF) of PTEs in mining soils of Ebonyi State, Nigeria

Site	Cd	Cr	Cu	Ni	Pb	Zn
AA	3.91	3.44	3.80	0.95	17.28	12.44
AB	1.13	2.74	2.50	0.67	8.04	6.01
NA	0.93	2.68	3.55	2.06	18.51	18.10
NB	2.64	2.31	3.04	2.00	15.01	10.48
IA	1.44	3.07	1.41	1.18	0.98	2.89
IB	2.45	3.45	1.70	2.66	3.91	2.56

Values represent mean EF (n = 20 per site). EF < 2 indicates minimal enrichment; 2–<5, moderate; 5–<20, significant; 20–<40, very high; and ≥ 40, extremely high enrichment. Fe was used as the reference element; results should be interpreted cautiously because Fe may not be geochemically conservative in mining soils.

Multivariate geochemical relationships and potential sources

Pearson's correlation analysis revealed significant associations among PTEs and soil properties (Table 4). Strong positive correlations between Pb–Zn (r = 0.67), Cu–Zn (r = 0.66) and Cu–Pb (r = 0.59; $p < 0.01$) suggest shared geochemical associations consistent with polymetallic mineralization in the Lower Benue Trough (Olade and Morton, 1985). Soil pH correlated negatively with Pb (r = −0.75), Zn (−0.64), Cu (−0.60), Ni (−0.51) and Cr (−0.49), suggesting greater PTE accumulation in acidic environments. Conversely, soil organic matter (SOM) correlated positively with Cu (r = 0.62), Zn (0.63) and Pb (0.56), while Fe showed positive associations with Pb and Zn (both r = 0.69). These relationships are consistent with sulfide weathering and potential metal retention by organic matter and Fe-bearing phases, although site-specific geological differences may also contribute [3, 39]. However, site-adjusted regression revealed no significant soil-property coefficients after Benjamini–Hochberg correction ($q \geq 0.05$), indicating that pooled correlations did not establish independent within-site geochemical controls. Principal component analysis (PCA) explained 80.68% of the total elemental variance through three components (Tables 11–12; Fig. 8). PC1 (54.95%) showed strong positive loadings for Zn (0.861), Pb (0.829), Cu (0.829) and Cr (0.718), representing a dominant multielement enrichment gradient consistent with Pb–Zn mineralization and mining-related disturbances. PC2 (14.87%) was dominated by Cd (0.854), suggesting a comparatively distinct distribution potentially associated with heterogeneous mineral assemblages or residual mine wastes. PC3 (10.86%) reflected contrasting Cr (0.592) and Ni (−0.441) associations, indicating additional geochemical variability. These patterns demonstrate the usefulness of PCA for identifying elemental associations, although individual components cannot independently establish contaminant sources [38].

Table 10.

Element-specific potential ecological risk factors (Er) of PTEs in mining soils of Ebonyi State, Nigeria

Site	Cd	Cr	Cu	Ni	Pb	Zn
AA	534.59	31.38	87.68	22.03	391.16	57.29
AB	126.71	18.46	47.78	11.28	214.64	19.32
NA	113.17	21.92	73.21	40.71	373.24	73.24
NB	185.22	10.13	34.60	23.17	154.19	23.56
IA	113.62	16.65	18.96	15.58	12.97	7.77
IB	145.46	13.32	16.32	25.12	35.04	4.80

Values represent mean element-specific potential ecological risk factors (n = 20 per site), calculated as Er = Tr × CF, using toxic-response factors of 30, 2, 5, 5, 5 and 1 for Cd, Cr, Cu, Ni, Pb and Zn, respectively. Er values indicate potential ecological.

The PCA scores (Fig. 9) further demonstrated site-specific geochemical differentiation. PERMANOVA confirmed significant multivariate differences among mining locations (pseudo-F = 24.26; $R^2 = 0.516$; $p = 0.0002$), with site identity accounting for approximately 51.6% of multielement variability. The dispersion test was not significant ($p = 0.141$), suggesting that differences in within-site dispersion did not provide a clear alternative explanation. Collectively, the correlation, PCA and PERMANOVA results indicate distinct geochemical signatures associated with mineralization and mining conditions, while Cd exhibited comparatively

independent variability. Nevertheless, the absence of significant site-adjusted regression coefficients limits definitive source attribution, highlighting the need for mineralogical and elemental speciation analyses to distinguish geological enrichment from mining-related contributions.

Table 11.

Principal component loadings of potentially toxic elements (PC1–PC3) in mining soils of Ebonyi State, Nigeria

Element	PC1	PC2	PC3
Cd	0.459	**0.854**	−0.200
Cr	**0.718**	−0.023	0.592
Cu	**0.829**	0.044	0.113
Ni	0.696	−0.392	−0.441
Pb	**0.829**	−0.061	−0.229
Zn	**0.861**	−0.102	0.081

Bold values indicate strong component loadings (|loading| ≥ 0.70). PC = principal component; PTEs = potentially toxic elements.

Table 12.

Total variance explained by principal component analysis of potentially toxic elements in mining soils

Principal component	Explained variance (%)	Cumulative variance (%)
PC1	54.948	54.948
PC2	14.868	69.816
PC3	10.860	80.676
PC4	7.782	88.458
PC5	6.565	95.022
PC6	4.978	100.000

The first three principal components collectively explained 80.68% of the total variance, with PC1 accounting for the largest proportion (54.95%).

Integrated contamination and potential ecological risks

The pollution load index (PLI) and modified degree of contamination (mCd) revealed substantial cumulative PTE contamination across the mining sites (Table 6; Figs. 2 and 10). All PLI values exceeded unity, with the highest recorded at AA (19.34 ± 5.09) and NA (15.23 ± 3.31), compared with lower values at IA (3.78 ± 0.92) and IB (4.09 ± 1.73). Similarly, mCd indicated extremely high contamination at AA (31.83 ± 10.33) and NA (30.90 ± 10.36), very high contamination at AB (14.59 ± 7.64) and NB (12.87 ± 5.22), and high contamination at the limestone sites (4.90–5.27). These patterns reflect pronounced Pb–Zn-associated enrichment in the mineralized districts and persistent contamination at abandoned locations. Comparable integrated index-based assessments have demonstrated the importance of combining multiple contamination indicators to characterize soil pollution [25]. Potential ecological risk indices (PERI) showed a similar spatial pattern (Table 6; Figs. 7 and 10), with the highest values at AA (1124.13 ± 406.73) and NA (695.48 ± 195.33), followed by AB (438.19 ± 238.64) and NB (430.87 ± 146.25). Lower values occurred

at IB (240.05 ± 94.43) and IA (185.54 ± 88.87), indicating comparatively greater potential ecological concern in the Pb–Zn mining environments. Element-specific ecological risk factors (Table 10) identified Cd and Pb as the dominant contributors. At AA, Cd and Pb accounted for approximately 47.6% and 34.8% of PERI, respectively, whereas Pb dominated at NA (53.7%). Conversely, Cd contributed approximately 61.2% and 60.6% at IA and IB, respectively. This variation demonstrates that ecological risk depends on both elemental enrichment and toxicity weighting, with Cd contributing disproportionately because of its high assigned toxic-response factor [12].

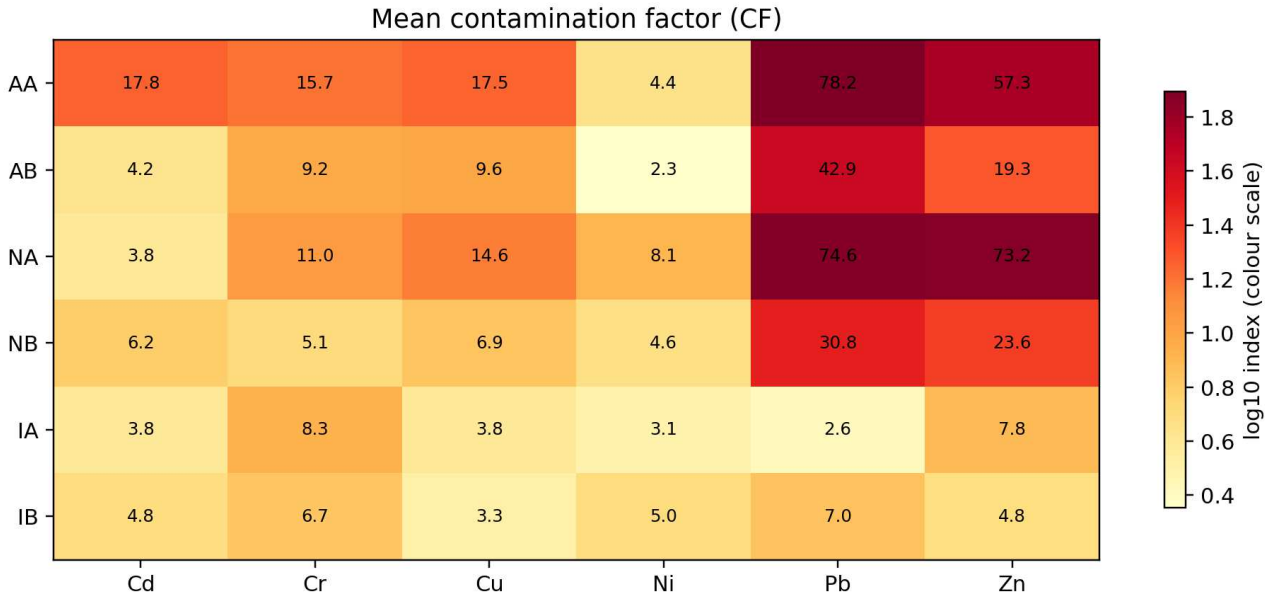


Fig. 4. Spatial differences in mean contamination factors; cell labels show untransformed CF.

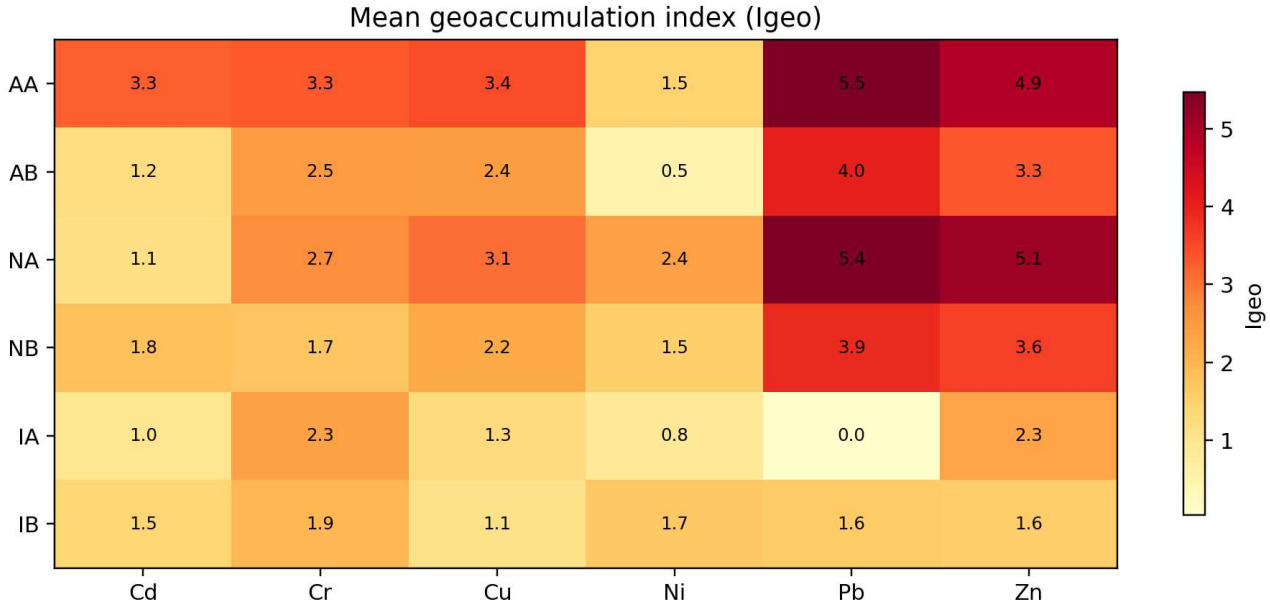


Fig. 5. Mean geoaccumulation indices for six potentially toxic elements.

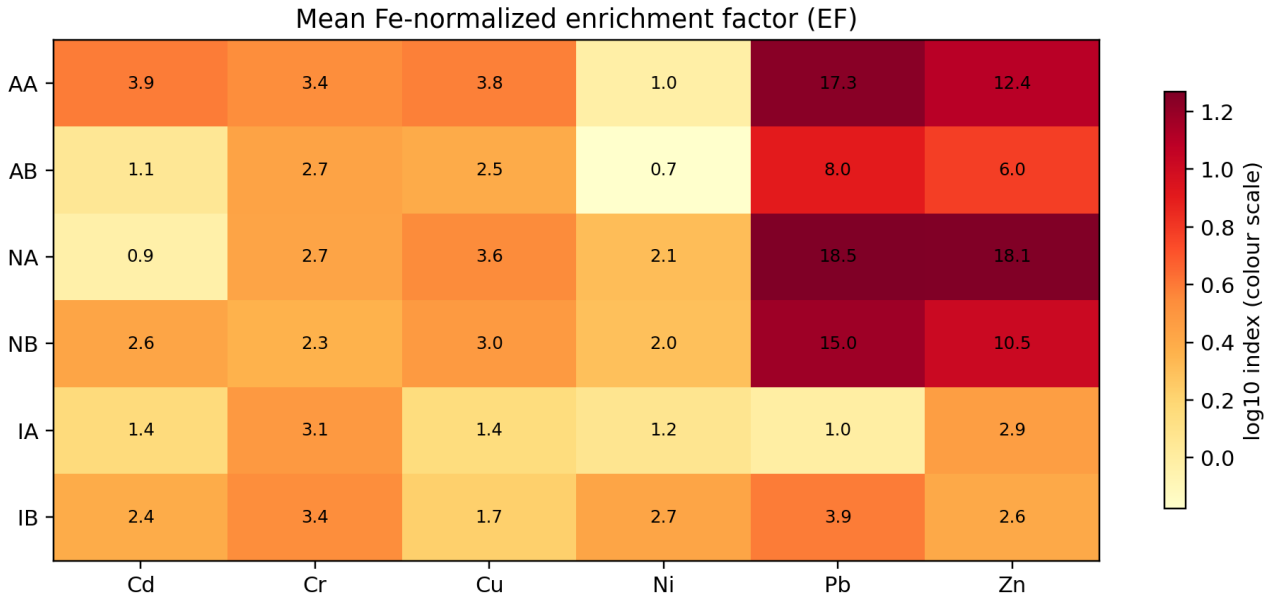


Fig. 6. Mean Fe-normalized enrichment factors.

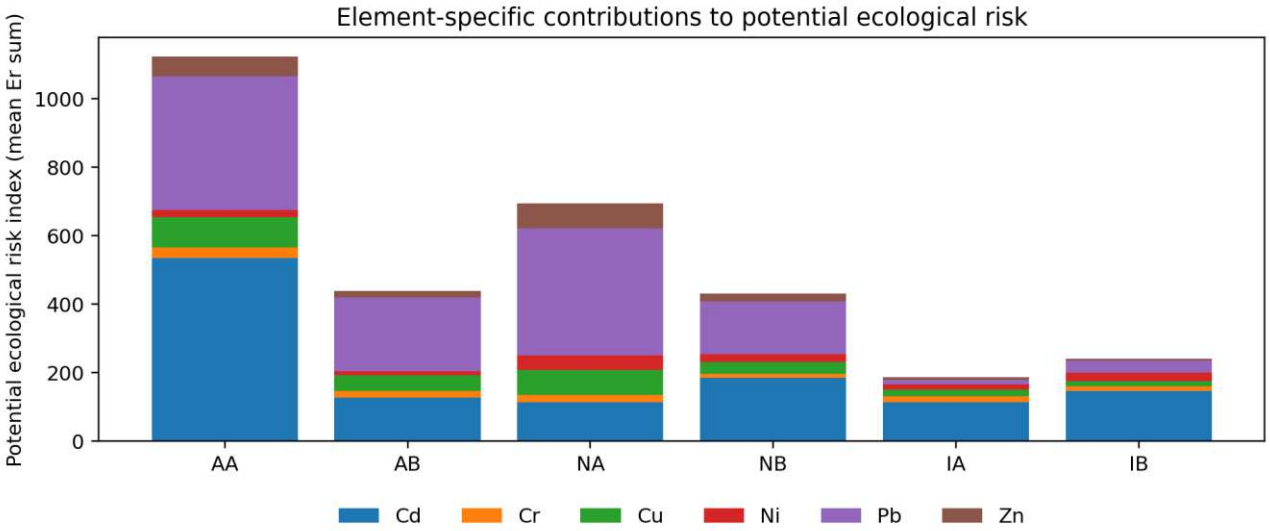
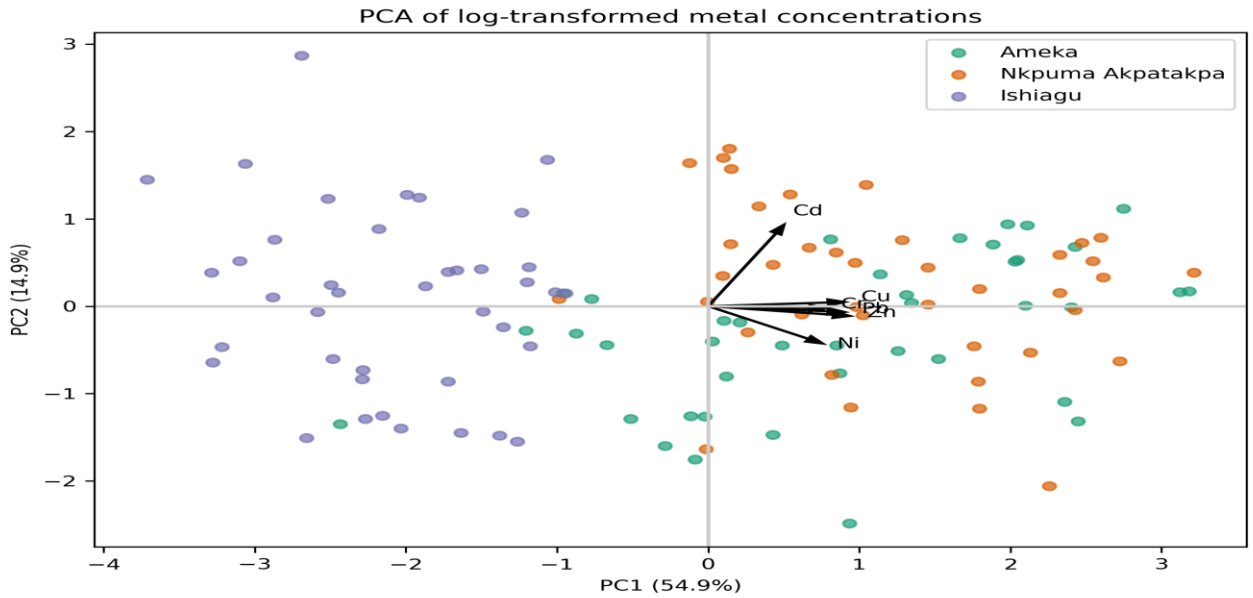


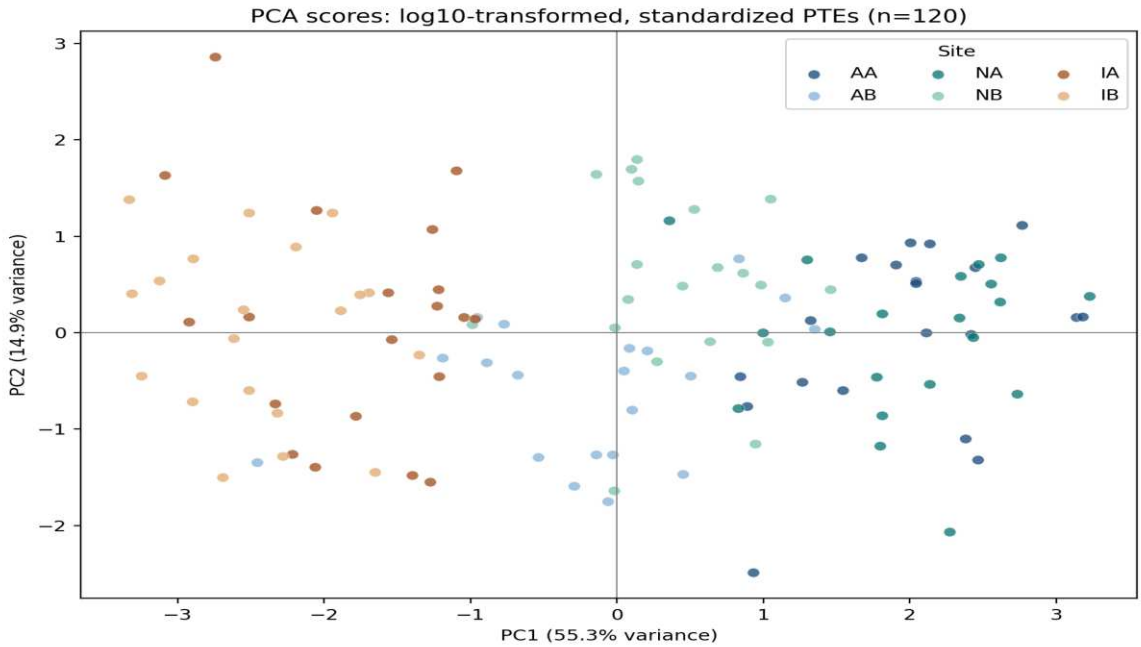
Fig. 7. Contributions of six elements to potential ecological risk across sites.

Although the contamination and ecological risk indices consistently identified AA and NA as priority locations, their interpretation depends on the selected geochemical backgrounds and toxic-response coefficients. Furthermore, the Håkanson framework was originally developed for aquatic sediments; its application to mining soils therefore provides comparative ecological screening rather than direct evidence of ecological damage. The substantial indices at abandoned locations suggest persistent legacy contamination, potentially sustained by mineral weathering and redistribution of residual mine wastes, consistent with observations from abandoned sulfide mining environments [2]. These findings highlight the need for targeted remediation and continued monitoring of both active and abandoned Pb–Zn mines, alongside surveillance of Cd contamination in limestone mining environments.



546

547 Fig. 8: Principal component analysis of log-transformed, standardized metal concentrations in 120
548 mining-soil samples.



549

550 Fig. 9. PCA scores for 120 mine-soil samples, coloured by sampling site. The PERMANOVA test compares
551 six sampling locations

552

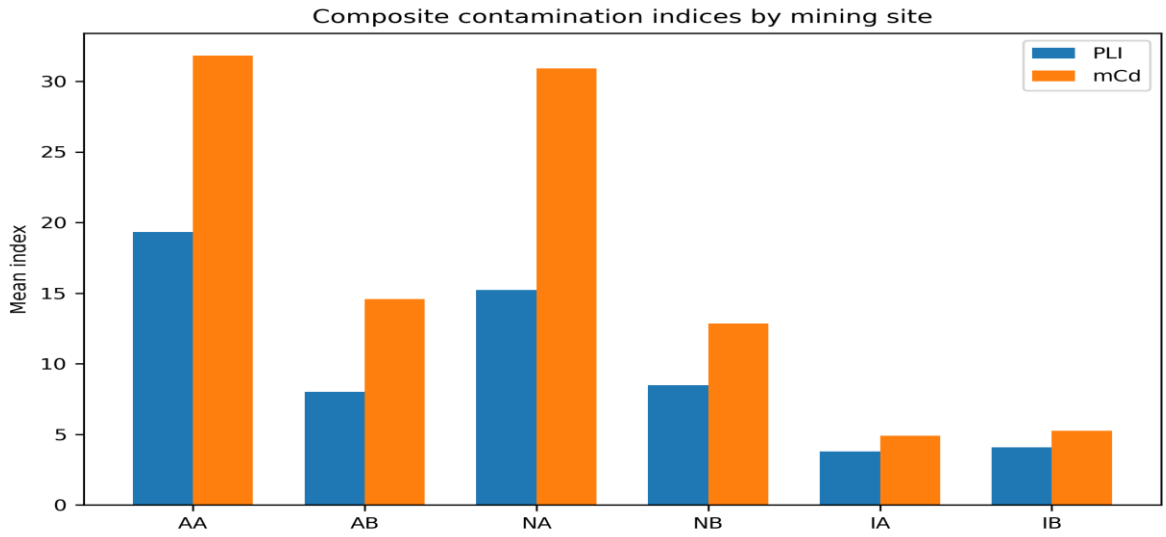


Fig. 10. Comparison of composite contamination and ecological-risk indices across mining sites.

Table 13.
Average daily dose (ADD) of Pb, Cd, Cr and Ni through soil ingestion in children and adults across the mining sites.

Site	Receptor	ADD (Pb)	ADD (Cd)	ADD (Cr)	ADD (Ni)
AA	Child	5.421E−02	2.076E−04	1.805E−03	1.266E−03
	Adult	5.808E−03	2.224E−05	1.934E−04	1.357E−04
AB	Child	2.467E−02	9.396E−05	1.125E−03	9.276E−04
	Adult	2.643E−03	1.007E−05	1.205E−04	9.938E−05
NA	Child	4.977E−02	1.976E−04	2.034E−03	1.304E−03
	Adult	5.333E−03	2.117E−05	2.179E−04	1.397E−04
NB	Child	2.265E−02	2.157E−04	1.092E−03	8.766E−04
	Adult	2.427E−03	2.311E−05	1.170E−04	9.392E−05
IA	Child	1.220E−03	1.162E−04	9.127E−04	6.759E−04
	Adult	1.307E−04	1.245E−05	9.779E−05	7.242E−05
IB	Child	3.179E−03	9.621E−05	7.026E−04	5.947E−04
	Adult	3.406E−04	1.031E−05	7.528E−05	6.371E−05

ADD, average daily dose (mg kg^{-1} body weight day^{-1}); AA and AB, Ameka active and abandoned mines; NA and NB, Nkpuma Akpatakpa active and abandoned mines; IA and IB, Ishiagu active and abandoned mines, respectively. Values represent site means (n = 20). Exposure parameters were soil ingestion rates of 200 and 100 mg day^{-1} and body weights of 15 and 70 kg for children and adults, respectively. Exposure frequency was 350 days year^{-1}, with durations of 6 and 30 years for children and adults, respectively. ADD estimates were based on total soil concentrations and non-carcinogenic averaging times.

Oral exposure and human health risk assessment

Estimated average daily doses (ADDs) through incidental soil ingestion varied across mining locations and receptor groups (Table 13). Children consistently exhibited higher exposure estimates than adults, reflecting their greater assumed soil ingestion rate relative to body weight (Moya et al., 2004). Lead dominated mass-based exposure in the Pb–Zn mining environments, with childhood ADDs reaching 5.421×10^{-2} and 4.977×10^{-2} mg kg^{-1} day^{-1} at AA and NA, respectively, compared with 1.220×10^{-3} mg kg^{-1} day^{-1} at IA. These differences reflect elevated Pb concentrations in mineralized soils and highlight potential exposure concerns. Similar investigations have emphasized the importance of soil and dust ingestion in mining communities, particularly among children [4].

Table 14.

Site-specific non-carcinogenic hazard indices and cumulative carcinogenic risk screening estimates associated with oral ingestion of potentially toxic elements in children and adults.

Site	Children HI	Adults HI	Children ΣCR*	Adults ΣCR*
AA	2.140	0.229	4.60E−02	2.47E−02
AB	0.987	0.106	2.20E−02	1.18E−02
NA	2.042	0.219	4.36E−02	2.34E−02
NB	2.201	0.236	2.05E−02	1.10E−02
IA	1.197	0.128	4.21E−03	2.25E−03
IB	0.992	0.106	4.88E−03	2.61E−03

HI, hazard index; ΣCR, cumulative carcinogenic risk screening index; AA, Ameka active mine; AB, Ameka abandoned mine; NA, Nkpuma Akpatakpa active mine; NB, Nkpuma Akpatakpa abandoned mine; IA, Ishiagu active mine; IB, Ishiagu abandoned mine. Values represent site means (n = 20). HI was calculated from the hazard quotients of Cd, Cr and Ni; Pb was excluded because no established oral reference dose is available (lead is classified as a probable human carcinogen, Group B2).

Non-carcinogenic risk assessment revealed higher partial oral hazard indices (HI) for children than adults (Tables 14 and 16; Fig. 11). Childhood HI ranged from 0.987 (AB) to 2.201 (NB), exceeding the screening threshold of unity at AA (2.140), NA (2.042), NB (2.201) and IA (1.197). Conversely, adult HI values remained below unity (0.106–0.236). Sample-level exceedances occurred in 75%, 35%, 80%, 80%, 50% and 45% of childhood samples at AA, AB, NA, NB, IA and IB, respectively, whereas no adult samples exceeded HI = 1. Notably, AB and IB exhibited mean HI values below unity despite appreciable sample-level exceedances, demonstrating the importance of within-site variability. These results indicate greater potential non-carcinogenic concern for children under the adopted exposure assumptions, although HI > 1 does not establish the occurrence of adverse health effects.

Table 15.

Site-specific lifetime-averaged carcinogenic risk screening indices for Pb, Cd, Cr and Ni through soil ingestion in children and adults.

Site	Receptor	CR (Pb)	CR (Cd)	CR (Cr)	CR (Ni)	ΣCR
AA	Adult	2.12E−02	5.81E−05	3.40E−03	4.88E−05	2.47E−02
	Child	3.95E−02	1.09E−04	6.34E−03	9.12E−05	4.60E−02
AB	Adult	9.63E−03	2.63E−05	2.12E−03	3.58E−05	1.18E−02
	Child	1.80E−02	4.91E−05	3.95E−03	6.68E−05	2.20E−02
NA	Adult	1.94E−02	5.53E−05	3.83E−03	5.03E−05	2.34E−02
	Child	3.63E−02	1.03E−04	7.15E−03	9.39E−05	4.36E−02
NB	Adult	8.84E−03	6.04E−05	2.06E−03	3.38E−05	1.10E−02
	Child	1.65E−02	1.13E−04	3.84E−03	6.31E−05	2.05E−02
IA	Adult	4.76E−04	3.26E−05	1.72E−03	2.61E−05	2.25E−03
	Child	8.89E−04	6.08E−05	3.21E−03	4.87E−05	4.21E−03
IB	Adult	1.24E−03	2.69E−05	1.32E−03	2.29E−05	2.61E−03
	Child	2.32E−03	5.03E−05	2.47E−03	4.28E−05	4.88E−03

CR, carcinogenic risk screening index; ΣCR, cumulative carcinogenic risk screening index. AA and AB, Ameka active and abandoned mines; NA and NB, Nkpuma Akpatakpa active and abandoned mines; IA and IB, Ishiagu active and abandoned mines, respectively. Values represent site means (n = 20; sampling depth: 5–10 cm). ΣCR is the sum of the four element-specific indices calculated using total soil concentrations and lifetime-averaged ingestion doses. All ΣCR values exceed the conventional upper screening benchmark of 1×10^{-4}.

Table 16.

Oral non-carcinogenic screening hazard index

Site	Children HI ± SD	Children n(HI > 1)	Adults HI ± SD	Adults n(HI > 1)
AA	2.140 ± 1.176	15	0.229 ± 0.126	0
AB	0.987 ± 0.571	7	0.106 ± 0.061	0
NA	2.042 ± 0.995	16	0.219 ± 0.107	0
NB	2.201 ± 1.156	16	0.236 ± 0.124	0
IA	1.197 ± 0.920	10	0.128 ± 0.099	0
IB	0.992 ± 0.512	9	0.106 ± 0.055	0

HI = HQ(Cd) + HQ(Cr) + HQ(Ni); Pb is not included. Mean ± sample SD (n = 20). HI > 1 indicates a screening concern under the specified assumptions, not observed disease.

Element-specific analysis identified Cd as the dominant contributor to partial oral HI (95.2–98.0%), followed by Ni (2.0–4.7%), while Cr contributed approximately 0.1% or less (Table 17; Fig. 12). Despite the substantially higher Pb and Zn concentrations, Cd dominated the calculated HI because of its relatively low adopted oral reference dose. However, Pb was excluded owing to the absence of an established health-protective oral reference dose, making the reported HI a partial risk estimate. Furthermore, Cr was measured without speciation, whereas the adopted reference dose applies to a particular Cr(III) form. Consequently, the relative contributions should be interpreted within these toxicological assumptions rather than as comprehensive rankings of health hazards.

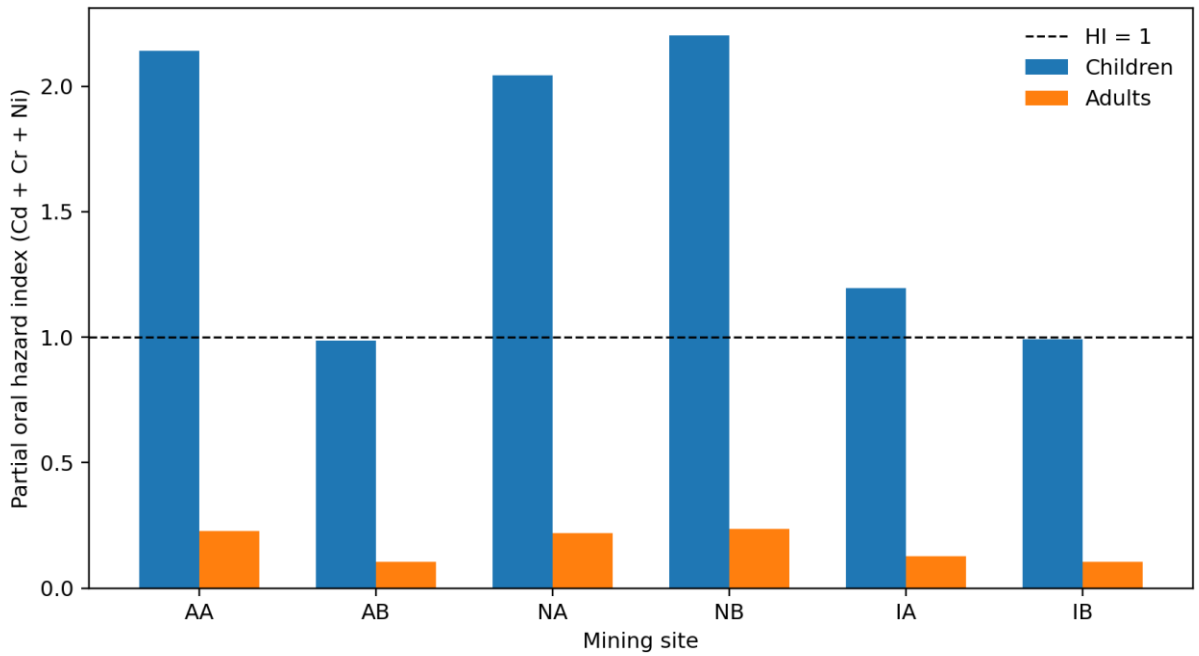


Figure 11. Comparison of mean partial oral hazard indices for children and adults. The dashed line denotes the conventional screening threshold of HI = 1.

Table 17.
Percentage contributions of PTEs to the partial oral hazard index (HI) and childhood risk exceedances.

Site	Cd (%)	Cr (%)	Ni (%)	Child HI	Child n > 1
AA	97.0	0.1	3.0	2.140	15
AB	95.2	0.1	4.7	0.987	7
NA	96.7	0.1	3.2	2.042	16
NB	98.0	0.0	2.0	2.201	16
IA	97.1	0.1	2.8	1.197	10
IB	97.0	0.0	3.0	0.992	9

HI = hazard index; Cd, Cr and Ni contributions represent their percentage contributions to the oral HI. Child HI represents the site-level hazard index for children; Child n > 1 indicates the number of soil samples exceeding HI = 1 (n = 20 per site). Values are rounded to one decimal place, so percentages may not sum exactly to 100%. Chromium contributions displayed as 0.0% represent values below 0.05%. Lead was excluded because an established oral reference dose was unavailable.

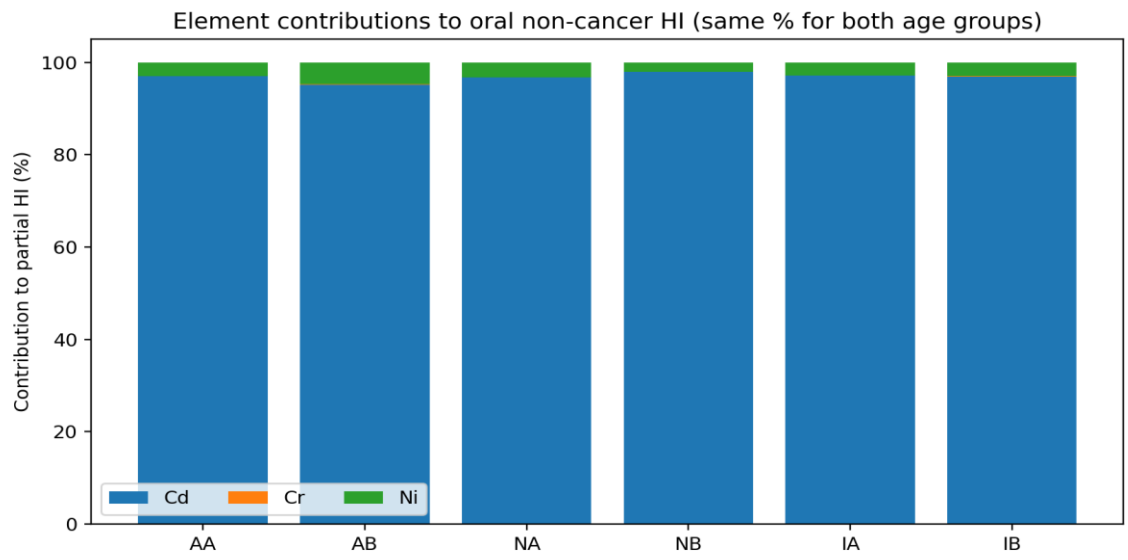


Fig. 12. Relative contributions of Cd, Cr and Ni to the oral non-carcinogenic hazard index across the six mining sites in Ebonyi State, Nigeria.

Provisional cumulative carcinogenic screening indices ranged from 4.21×10^{-3} to 4.60×10^{-2} for children and 2.25×10^{-3} to 2.47×10^{-2} for adults (Tables 14–15), with the highest values at AA and NA. However, the applicability of the adopted oral cancer slope factors to the measured forms of Pb, Cd, Cr and Ni remains unverified. These estimates therefore represent preliminary model outputs rather than validated lifetime cancer probabilities. Additionally, exposure calculations were based on pseudo-total concentrations rather than gastrointestinally bioaccessible fractions, potentially limiting their representation of biological exposure [2, 5, 16]. The findings generally, identify AA and NA as major contamination and ecological-risk hotspots, while NB exhibited the highest childhood HI, demonstrating that contamination intensity does not necessarily correspond to toxicity-weighted human health risk. Persistent contamination at abandoned locations further emphasizes the need for targeted remediation, dust-exposure control and continued environmental monitoring. Future assessments incorporating oral bioaccessibility, Cr speciation, and biological exposure indicators would strengthen the evaluation of potential health implications for surrounding communities.

Conclusion

This study provides an integrated assessment of geochemical contamination, potential sources, ecological risks and human health implications of potentially toxic elements in active and abandoned Pb–Zn and limestone mining soils of Ebonyi State, Nigeria. The findings revealed pronounced spatial variability, with Pb–Zn mining environments exhibiting substantially greater PTE accumulation than limestone locations. Active Ameka (AA) and Nkpuma Akpatakpa (NA) recorded the highest cumulative contamination and ecological risk indices, while significant active–abandoned differences in 13 of 18 elemental comparisons demonstrated the influence of site-specific mining conditions. Nevertheless, substantial contamination at abandoned locations highlights the persistence of legacy mine pollution.

Multivariate analyses identified strong Pb–Zn–Cu associations consistent with regional polymetallic mineralization, while Cd exhibited a comparatively distinct distribution. PERMANOVA confirmed significant geochemical differentiation among sites ($R^2 = 0.516$; $p = 0.0002$), although site-adjusted regression provided insufficient evidence to establish independent soil-property controls. Ecological risk was predominantly associated with Cd and Pb, whereas Cd contributed 95.2–98.0% of the calculated partial oral hazard index. Children exhibited greater potential non-carcinogenic concern than adults, with mean hazard indices exceeding unity at four locations and the highest value occurring at the abandoned Nkpuma Akpatakpa mine (NB). These findings demonstrate that contamination magnitude, ecological risk and human health screening outcomes do not necessarily follow identical spatial patterns. The study highlights the importance of integrating geochemical indices, multivariate statistics and receptor-specific risk assessment to identify environmental priorities in mining-affected regions. Priority interventions should include containment and rehabilitation of contaminated mine wastes, control of soil and dust dispersion, and sustained monitoring of both active and abandoned mining locations. Further investigations incorporating metal speciation, oral bioaccessibility and validated exposure models are recommended to refine source attribution and human health risk estimates. The findings provide a scientific basis for targeted remediation, improved mine-site management and evidence-based environmental protection in southeastern Nigeria.

Funding

This research was funded by the Tertiary Education Trust Fund (TETFund) (NMU/TETFUND/2022/081) and the Petroleum Technology Development Fund (PTDF/ED/ISS/PHD/JSN/0057/2323ISSPHD0057). The authors also gratefully acknowledge financial support from the Ebonyi State Research Scholarship Fund.

Author Contributions

Nworu Jerome Sunday and Elom I. Nwabueze contributed to the study conception, study design and material preparation. Data collection and analysis were performed by Nworu A. Ursula, Edith A. Enemose and Arisabor Lucky. Laboratory analysis and the first draft of the manuscript were completed by Nworu S. Jerome. All authors have read and given approval for the final manuscript.

Data Availability

All datasets generated and analysed in this study are provided within the article and its Supplementary Information. Further supporting data are available from the corresponding author upon reasonable request.

Competing Interests

The authors declare no competing interests.

Declarations

Clinical trial number: Not applicable.

Ethics, Consent to Participate, and Consent to Publish declarations: Not applicable.

References

1. Kumar S, Anshumali (2025) Heavy metal pollution and health risk assessment in upland and riparian soils of the Ganga River basin. Discover Soil 2:33. https://doi.org/10.1007/s44378-025-00061-4

2. Cánovas CR, Quispe D, Macías F, Callejón-Leblic B, Arias-Borrego A, García-Barrera T, Nieto JM (2023) Potential release and bioaccessibility of metal/loids from mine wastes deposited in historical abandoned sulfide mines. Environmental Pollution 316:120629. https://doi.org/10.1016/j.envpol.2022.120629

3. Alloway BJ (2013) Heavy Metals in Soils: Trace Metals and Metalloids in Soils and Their Bioavailability, 3rd edn. Springer, Dordrecht. https://doi.org/10.1007/978-94-007-4470-7

4. He A et al. (2020) Potentially toxic metals and the risk to children's health in a coal mining city: An investigation of soil and dust levels, bioaccessibility and blood lead levels. Environment International 141:105788. https://doi.org/10.1016/j.envint.2020.105788

5. Cocerva T et al. (2024) Using oral bioaccessibility measurements to refine risk assessment of potentially toxic elements in topsoils across an urban area. Ecotoxicology and Environmental Safety 276:116293. https://doi.org/10.1016/j.ecoenv.2024.116293

6. Naz M et al. (2022) The soil pH and heavy metals revealed their impact on soil microbial community. Journal of Environmental Management 321:115770. https://doi.org/10.1016/j.jenvman.2022.115770

7. Ruby MV et al. (1999) Advances in evaluating the oral bioavailability of inorganics in soil for use in human health risk assessment. Environmental Science & Technology 33:3697–3705. https://doi.org/10.1021/es990479z

8. Mufalo W et al. (2024) Insights on hazardous metal bioaccessibility, and groundwater impacted by Zn residues from a legacy mine and risk evaluation of adjacent soils. Environmental Geochemistry and Health 46:64. https://doi.org/10.1007/s10653-024-01864-0

9. Ozobialu B, Igwe O, Emeh C (2020) Lateral distribution of potential toxic elements from lead–zinc mine sites within Enyigba, Southeastern Nigeria. Environmental Earth Sciences 79:378. https://doi.org/10.1007/s12665-020-09122-z

10. Müller G (1969) Index of geoaccumulation in sediments of the Rhine River. GeoJournal 2:108–118.

11. Sutherland RA (2000) Bed sediment-associated trace metals in an urban stream, Oahu, Hawaii. Environmental Geology 39:611–627. https://doi.org/10.1007/s002540050473

12. Håkanson L (1980) An ecological risk index for aquatic pollution control: A sedimentological approach. Water Research 14:975–1001. https://doi.org/10.1016/0043-1354(80)90143-8

13. US EPA (1989) Risk Assessment Guidance for Superfund, Volume I: Human Health Evaluation Manual (Part A). EPA/540/1-89/002. Washington, DC.

14. US EPA (2001) Risk Assessment Guidance for Superfund, Volume I: Human Health Evaluation Manual (Part E, Supplemental Guidance for Dermal Risk Assessment).

15. Moya J, Bearer CF, Etzel RA (2004) Children's behavior and physiology and how it affects exposure to environmental contaminants. Pediatrics 113:996–1006.

16. Wragg J et al. (2011) An inter-laboratory trial of the Unified BARGE bioaccessibility method for arsenic, cadmium and lead in soil. Science of the Total Environment 409:4016–4030. https://doi.org/10.1016/j.scitotenv.2011.05.019

17. Joint FAO/WHO Expert Committee on Food Additives (2011) Evaluation of Certain Food Additives and Contaminants: Seventy-third Report. WHO Technical Report Series 960. World Health Organization, Geneva.

18. US EPA (2024) IRIS Toxicological Review of Hexavalent Chromium [Cr(VI)]. EPA/635/R-24/164. United States Environmental Protection Agency, Washington, DC.

19. Asamoah BD et al. (2023) Distribution and in-vitro bioaccessibility of potentially toxic metals in surface soils from a mining and a non-mining community in Ghana: Implications for human health. Environmental Geochemistry and Health 45:9875–9889. https://doi.org/10.1007/s10653-023-01776-5

20. Olade MA, Morton RD (1985) Origin of lead-zinc mineralization in the southern Benue Trough, Nigeria—fluid inclusion and trace element studies. Mineralium Deposita 20:76–80. https://doi.org/10.1007/BF00204313

21. Umeobi EC et al. (2024) Evaluation of potentially toxic elements in soils developed on limestone and lead-zinc mine sites in parts of southeastern Nigeria. Heliyon 10:e27503. https://doi.org/10.1016/j.heliyon.2024.e27503

22. Obasi PN, Akudinobi BB (2020) Potential health risk and levels of heavy metals in water resources of lead–zinc mining communities of Abakaliki, southeast Nigeria. Applied Water Science 10:184. https://doi.org/10.1007/s13201-020-01233-z

23. Akakuru OC et al. (2024) Carcinogenic health risks and water quality assessment of groundwater around lead–zinc mining areas of Ebonyi State Nigeria: A data-driven machine learning approach. Discover Civil Engineering 1:130. https://doi.org/10.1007/s44290-024-00134-3

24. Kicińska A, Pomykała R, Izquierdo-Diaz M (2022) Changes in soil pH and mobility of heavy metals in contaminated soils. European Journal of Soil Science 73. https://doi.org/10.1111/ejss.13203

25. Udo, B. U., Udosen, N. I., and Ibia, T. O. (2026). Comprehensive geochemical characterization and multi-index ecotoxicological appraisal of heavy metal contamination in soils impacted by open waste disposal practices. Discover Soil, 3, Article 17. https://doi.org/10.1007/s44378-026-00177-1

26. International Organization for Standardization (ISO). (2002). ISO 10381-1:2002: Soil quality—Sampling—Part 1: Guidance on the design of sampling programmes. ISO, Geneva.

27. International Organization for Standardization (ISO). (1995). ISO 11466:1995: Soil quality—Extraction of trace elements soluble in aqua regia. ISO, Geneva.

28. International Organization for Standardization (ISO). (2021). ISO 10390:2021: Soil, treated biowaste and sludge—Determination of pH. Geneva: ISO. Official ISO standard.

29. Soil Survey Staff. (2014). Soil Survey Field and Laboratory Methods Manual. Soil Survey Investigations Report No. 51, Version 2.0. USDA Natural Resources Conservation Service. USDA methods manual.

30. Walkley, A., & Black, I. A. (1934). An examination of the Degtjareff method for determining soil organic matter, and a proposed modification of the chromic acid titration method. Soil Science, 37(1), 29–38. https://doi.org/10.1097/00010694-193401000-00003.

31. Chen M, Ma LQ (2001) Comparison of three aqua regia digestion methods for twenty Florida soils. *Soil Science Society of America Journal* 65(2):491–499. https://doi.org/10.2136/sssaj2001.652491x

32. Tomlinson, D. L., Wilson, J. G., Harris, C. R., & Jeffrey, D. W. (1980). Problems in the assessment of heavy-metal levels in estuaries and the formation of a pollution index. Helgoländer Meeresuntersuchungen, 33, 566–575. https://doi.org/10.1007/BF02414780

33 Abrahim, G. M. S., & Parker, R. J. (2008). Assessment of heavy metal enrichment factors and the degree of contamination in marine sediments from Tamaki Estuary, Auckland, New Zealand. Environmental Monitoring and Assessment, 136, 227–238. https://doi.org/10.1007/s10661-007-9678-2

34. Sutherland, R. A., Tolosa, C. A., Tack, F. M. G., & Verloo, M. G. (2000). Characterization of selected element concentrations and enrichment ratios in background and anthropogenically impacted roadside areas. Archives of Environmental Contamination and Toxicology, 38, 428–438. https://doi.org/10.1007/s002449910057.

780 35. Reimann, C., & de Caritat, P. (2000). Intrinsic flaws of element enrichment factors (EFs) in environmental
781 geochemistry. Environmental Science & Technology, 34(24), 5084–5091. https://doi.org/10.1021/es001339o.

782 36. Reimann, C., & de Caritat, P. (2005). Distinguishing between natural and anthropogenic sources for elements in
783 the environment: Regional geochemical surveys versus enrichment factors. Science of the Total Environment, 337(1–
784 3), 91–107. https://doi.org/10.1016/j.scitotenv.2004.06.011

785 37. Reimann, C., Filzmoser, P., Garrett, R. G., & Dutter, R. (2008). Statistical data analysis explained: Applied
786 environmental statistics with R. John Wiley & Sons. https://doi.org/10.1002/9780470987605.

787 38. Jolliffe, I. T., & Cadima, J. (2016). Principal component analysis: A review and recent developments.
788 Philosophical Transactions of the Royal Society A: Mathematical, Physical and Engineering Sciences, 374(2065),
789 20150202. https://doi.org/10.1098/rsta.2015.0202.

790 39. Reimann, C., Filzmoser, P., & Garrett, R. G. (2002). Factor analysis applied to regional geochemical data:
791 Problems and possibilities. Applied Geochemistry, 17(3), 185–206. https://doi.org/10.1016/S0883-2927(01)00066-X.

792 40. Mohammadi AA, Zarei A, Majidi S, Ghaderpoury A, Hashempour Y, Saghi MH, Alinejad A, Yousefi M,
793 Hosseingholizadeh N, Ghaderpoori M. Carcinogenic and non-carcinogenic health risk assessment of heavy metals in
794 drinking water of Khor ramabad. Iran MethodsX. 2019;6:1642–51. https://doi.org/10.1016/j.mex.2019.07.017.

Supplementary Files

This is a list of supplementary files associated with this preprint. Click to download.

- SupplementaryData.docx